PHYSICAL REVIEW B VOLUME 16, NUMBER 5 1 SEPTEMBER 1977

Electron tunneling study of the superconducting proximity effect in Pb-Cd†

J. R. Toplicar* and D. K. Finnemore
Ames Laboratory–ERDA and Department of Physics, Iowa State University, Ames, Iowa 50011
(Received 12 October 1976)

Electron tunneling has been used to study the superconducting state in superimposed Pb-Cd thin films in which the Pb thickness varied from 950 to 330 Å. The measured transition temperature T_c varied from 7.22 to 4.86 K in the samples, and the observed energy gaps varied from 1.38 to 0.43 meV. The tunneling density of states as recorded on either side of the sandwich resembles those predicted by the McMillan model, but there are some quantitative differences. The observed phonon structure in the density of states occurs at the same energy as that in bulk Pb, and the magnitude of the structure scales with T_c^2. The shape of the calculated phonon spectral function remains essentially unchanged throughout this series.

I. INTRODUCTION

Electron tunneling provides a powerful tool for the study of the proximity effect.[1-6] Differential conductance curves for a metal-oxide-superconductor junction are a sensitive probe of the superconducting density of states[7] $N(\omega)$ and, through $N(\omega)$, a great deal can be learned about the fundamental interactions in a superconductor.[8] For example, the transition temperature T_c, the energy gap Ω, and the position of the structure related to phonon peaks are measured directly. In addition, the energy-dependent pair potential $\Delta(\omega)$, the lifetime-broadening parameter Γ, and the effective electron-phonon coupling function $\alpha^2(\omega)F(\omega)$ are indirectly related to $N(\omega)$ and can be determined from the data.[8]

Proximity sandwiches differ from homogeneous superconducting films in several important respects.[9,10] If a normal metal is placed in intimate contact with a superconductor, electrons can flow from one metal to the other and one expects that there will be a characteristic escape time associated with both electrons on the superconducting side leaking into the normal region and the reverse process. Hence there will be a lifetime-broadening term Γ_S associated with a residence time in the superconducting side, and Γ_N, associated with a residence time on the normal side. Because the fundamental interactions have a spatial variation, one would expect the pair potential to depend on position as well.

For the films described here, electrons traveling at the Fermi velocity will cross the sample in about 10^{-13} sec, which is shorter than either the inverse gap time or the time of a single-phonon oscillation. In addition, for the films reported here, electrons incident on the superconductor–normal-metal interface in these films have a rather high chance of transmission, about 10%. Therefore, it is essential to think of these proximity composites as a strongly coupled unit.

Pb-Cd was chosen for a study of the proximity effect for a number of reasons. The transition temperature T_c is high and the strength of the electron-phonon interaction is such that strong-coupling effects are easily observed. In addition, the solubility of Pb in Cd is less than 0.2 at.% and the solubility of Cd in Pb is about 1.0 at.%, so the interdiffusion is not too serious a problem. Most important, however, is that we have learned to grow bulk samples of composite Pb-Cd structures[11] with oriented lamina and we wish to study flux pinning at a superconductor–normal-metal interface. These tunneling measurements are essential to our understanding of these flux pinning processes.

II. EXPERIMENTAL

Tunnel junctions of the form Al-Al_2O_3-Pb-Cd were prepared in a liquid-nitrogen trapped oil diffusion pump vacuum system. A complete description of sample preparation is given elsewhere,[12] so a brief account will suffice here. A fused-quartz substrate was cleaned sequentially in acetone, NaOH, and aqua regia. It was then boiled in Decontam detergent, rinsed in isopropanol, and dried in a stream of nitrogen gas. Gold contacts were deposited by evaporation and indium was soldered onto the edges of the film. A 0.005-cm wire was attached to one gold contact to provide an electrical ground. The substrate was then mounted in the vacuum system and the evaporation boats were outgassed with the shutter closed. An Al film approximately 2.5 cm long, 0.04 cm wide, and 1000 Å thick was deposited at a rate of 7 Å/sec as determined by the quartz-thickness monitor. After the Al deposition, a SiO film approximately 700 Å thick was deposited at 10 Å/sec over all portions except two cross strips 0.04 cm wide. At this point in the preparation,

50 μm of oxygen gas was introduced into the chamber and the Al_2O_3 barrier was grown in a glow discharge with the Al film at ground potential. The vacuum system was then opened to the atmosphere for about 3 min to permit installation of the Pb and Cd evaporation sources and masks and the system was then re-evacuated. The Pb and Cd were evaporated in quick succession to provide as intimate contact as possible. In a vacuum of 10^{-6} Torr, a monolayer of oxide could form in a few tens of seconds and we expect that some oxide does form during the 20- to 30-sec interval between the Pb and Cd evaporations. We have found that Cd sticks to a freshly evaporated Pb film fairly well, but some care is required to get Cd to stick to Al_2O_3 when the Al-Al_2O_3-Cd-Pb junctions were prepared. To solve this problem, the Cd evaporation boat was kept as cool as possible, approximately 250 °C, and a series of baffles was used to collimate the Cd beam. Even with these precautions, only about 20% of the Al-Al_2O_3-Cd-Pb junctions displayed the mirrorlike surfaces and good electrical properties needed for the experiment. Thicknesses of the films were measured optically to an accuracy of about 50 Å.

Dynamical conductance measurements were made in a standard ^{3}He refrigerator using the feedback method proposed by Rogers.[13] Modulation voltages were typically 30 μV in the gap region and 50 μV in the phonon-structure region. Temperatures were measured using a germanium thermometer GR1592 which had previously been calibrated against the T-58 vapor-pressure scale and cerium magnesium nitrate susceptibility scale.

III. RESULTS AND DISCUSSION

Tunnel junctions for this experiment always were made in pairs so that each proximity junction Al-Al_2O_3-Pb-Cd had a second control junction Al-Al_2O_3-Pb which was made in the same evaporation. The control junction provided a direct contrast to illustrate the effects arising from the Cd backing and it provided a measure of the Al energy gap. Our primary goal in this work was to study changes in the superconductivity of Pb caused by the presence of Cd so most of the junctions were of the form Al-Al_2O_3-Pb-Cd (hereafter called Pb-Cd films). We also were interested, however, in the pair potential on the Cd side so another family of junctions of the form Al-Al_2O_3-Cd-Pb (hereafter called Cd-Pb films) was also prepared.

For the family of Pb-Cd films, the thickness of the Pb, d_S, ranged from 950 to 330 Å and the thickness of the Cd, d_N, was held approximately constant at 500 Å as shown in Table I. Values of the superconducting parameters such as T_c and Ω are smoothly depressed as d_S decreases and the junction behavior is completely regular. Probably the best indication of the quality of the oxide barrier for these junctions is the resistance of the junction at zero bias R_0 when the temperature is low enough to show an energy gap. As shown in Table I, all junctions reported here have R_0 greater than 150 000 Ω. The normal-state resistance of the junctions at 77 K, R_N, is typically 50 to 1000 Ω and this means that leakage currents are less than 1% of the tunneling currents. The capacitance of the junctions is on the order of .01 μF which is consistent with a barrier thickness on the order of 20 Å. The quality of all the junctions reported here seem to be quite good.

A. Transition temperature

T_c for the Pb-Cd proximity sandwiches is depressed when compared to that of an unbacked Pb film. For example, the 670-Å proximity sandwich has a T_c of 6.27 K, whereas the corresponding unbacked Pb film has a T_c of 7.22 K. The transition temperatures were determined from the temperature dependence of the normalized tunneling conductance measured at zero-bias voltage.

TABLE I. Summary of tunnel-junction characteristics.

Sample	d_S (Å)	d_N (Å)	R_N (Ω)	R_0 (Ω)	T_c (K)	Ω (meV)	E_p (meV)	Γ_S (meV)	Γ_N (meV)	Δ_S^{Ph} (meV)	Δ_N^{Ph} (meV)
Pb	670	...	1240	307 000	7.22	1.38	1.38	0	...	...	...
Pb-Cd	950	470	2250	585 000	6.61	0.93	1.27	0.08	0.42	1.23	0.18
Pb-Cd	670	460	1050	378 000	6.27	0.72	1.22	0.13	0.49	1.15	0.25
Pb-Cd	500	460	172	265 000	5.85	0.57	1.07	0.18	0.52	1.04	0.40
Pb-Cd	330	520	253	236 000	4.86	0.43	0.73	0.32	0.54	0.72	0.56
Cd-Pb	650	1200	231	148 000	4.46	0.33	0.68	0.38	0.53	0.93	0.77
Cd-Pb	880	830	48	172 000	5.88	0.38	0.59	0.16	0.25	1.08	0.40
Cd	...	...	52	168 000	0.56	0.075	0.075	0	...	...	...

$$\sigma(0) = \left(\frac{dI}{dV}\right)_S \Big/ \left(\frac{dI}{dV}\right)_N \Bigg|_{V=0}.$$

The quantity $1-\sigma(0)$ is plotted vs temperature as shown in Fig. 1. These curves are linear in temperature near T_c and the critical temperature is determined by linearly extrapolating the $1-\sigma(0)$ curve to zero.

In broad outline, the dependence of T_c on d_S is in rather good agreement with previous proximity studies[5,14] as shown in Fig. 2. Both the Pb-Pt data of Hauser *et al.*[3] and the Pb-Ag data of Claeson and Gygax[5] are close to these Pb-Cd data. Attempts to fit the data to the de Gennes–Werthamer theory[9] show qualitative agreement but there may be quantitative difficulties. A family of T_c vs d_S curves calculated from the theory for various choices of the coherence distances, ξ_N and ξ_S, are shown on Fig. 2 by the dashed curve, the solid curve, and the dot-dash curve. Good agreement is found for $\xi_N = 500$ Å and $\xi_S = 150$ Å. On the basis of resistivity measurements, however, we believe that the mean free path in the Pb, l_S, is about 100 to 300 Å and this would give a coherence distance ξ_S of about 500 Å. As shown in Fig. 2, a value of $\xi_S = 500$ Å would give significant deviation between theory and experiment. It may be that the theory is inadequate to describe these films or, on the other hand, it may be that the coherence distance in the region of the junction really is only about 150 Å and that the film resistivity does not give a good measure of the mean free path in the junction area.

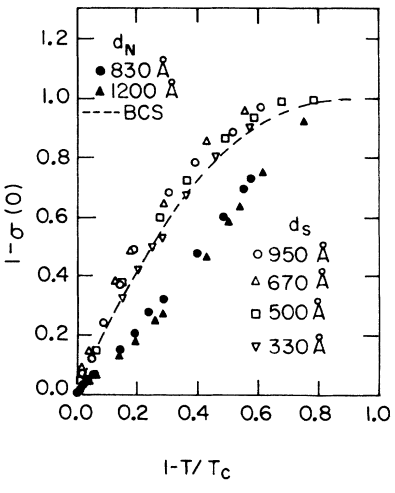

FIG. 1. Temperature dependence of the zero-bias tunnel conductance for both Pb-Cd (open symbols) and for Cd-Pb (solid symbols).

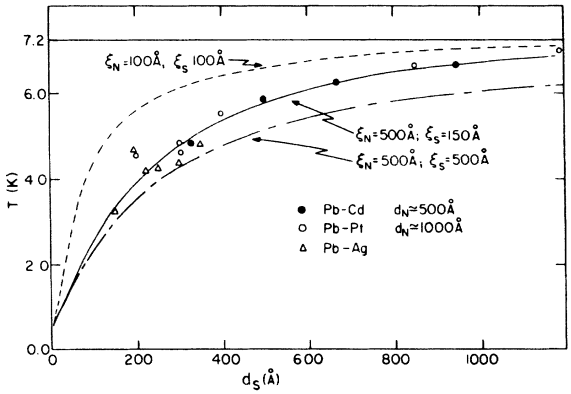

FIG. 2. Variation of transition temperature of the proximity sandwiches as a function of the thickness of the superconducting film. The solid, dashed, and dot-dash curves are based on the de Gennes-Werthamer theory for various choices of coherence distances ξ_N and ξ_S.

B. Electron density of states near the gap edge

For energies near the gap edge, the most prominent differences between the proximity sandwiches and the unbacked films are the lifetime-broadening effects associated with the ability of electrons in the Pb region to escape into the Cd region. As shown for the 330-Å junction at 0.34 K in Fig. 3(a), there is a very well-defined energy gap out to 0.6 meV with leakage currents less than 0.2% of the normal currents. At 0.6 meV σ rises rapidly and goes through a broad peak which is vaguely similar to the peaks for samples which show lifetime broadening due to magnetic impurities.[15,16] The data, however, differ from the density of states expected from the Abrikosov-Gor'kov (AG) theory for magnetic impurities[17] in that the theory predicts a much steeper rise in σ near the gap edge than is seen in the data. In fact the data in this regard are closer to the McMillan tunneling model (MTM)[10] for proximity sandwiches. In an attempt to understand these data in more detail, we have fit the results to MTM for each of the films. The lifetime-broadening parameters of the model, Γ_N and Γ_S, were determined from T_c of the sandwich, the bulk transition temperature T_{cb}, the density of states $N(0)$, and the thicknesses d_N and d_S using the McMillan equations. In making the fit to the data, there is one adjustable parameter Δ_S^{Ph}, which we have adjusted to put the theoretical peak in the density of states at same energy as the measured peak. With this one adjustable parameter all the other features of the density of states can be calculated from the theory. As is shown in Fig. 3(a), theory predicts Ω rather well for the 330-Å film, but the experimental peak is

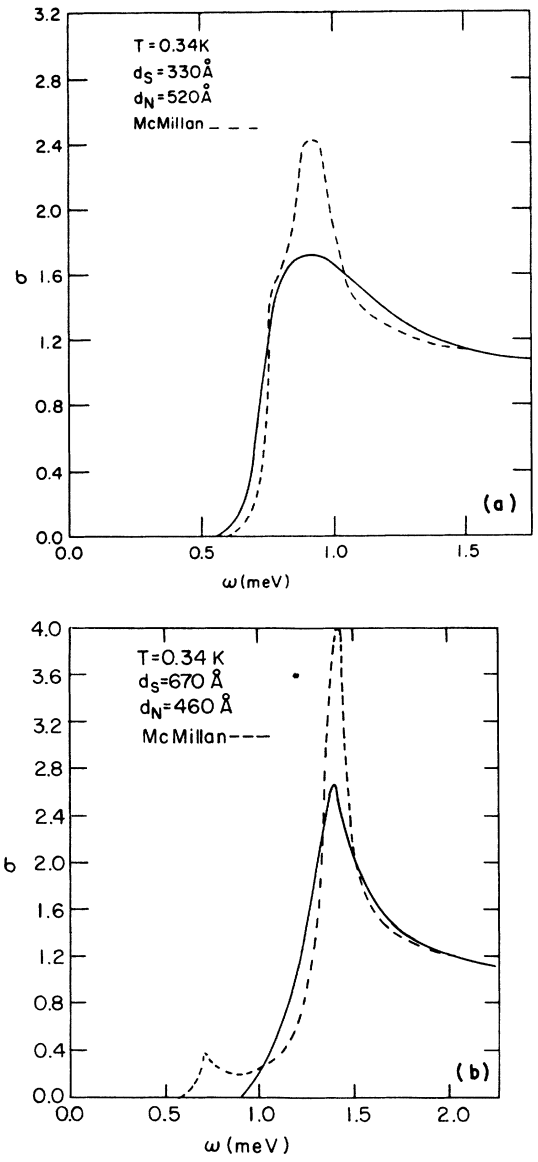

FIG. 3. Electron tunneling conductance near the gap edge for the 330- and the 670-Å films. The solid-line curve is the experimental result and is reproducible to the width of the line. The dashed curve is a McMillan model prediction for the parameters of this film. Energies are measured from the Fermi level.

somewhat more rounded than predicted. However, the general shape of the theoretical curve resembles the measurements. For all the thicker films, however, the agreement with MTM is not as good in the region just above Ω. As shown for the 670-Å film on Fig. 3(b), the theory predicts a substantial density of states at low energy associated with the Cd side of the film, but these states are not present in the data. Failure to see these states in the data may arise because the mean free path is much smaller than the sample thickness, whereas the theory assumes long mean free paths. At present, however, we have no quantitative explanation for the discrepancy. Similar studies of σ near the gap edge by Vrba and Woods[2] for Sn-Al junctions with an oxide barrier between the Sn and Al regions have shown the low-energy peaks as predicted by MTM so the theory is probably correct where the coupling between the superconducting and normal regions is weak. For the Pb-Cd films reported here, the probability of transmission across the barrier is about 0.1, so the films are relatively strongly coupled and the conditions of MTM are not as well satisfied.

Near T_c the density of states for both Pb-Cd and Cd-Pb are rather well behaved. As shown on Fig. 1, the value of $1-\sigma(0)$ for all the Pb-Cd films is rather close to the Bardeen-Cooper-Schrieffer (BCS)[18] prediction. The quantity $1-\sigma(0)$ is proportional to the square of the pair potential[4] so the linear behavior of $1-\sigma(0)$ implies that the pair potential varies as $(1-T/T_c)^{1/2}$ near T_c. Figure 1 shows the behavior of this parameter for tunneling into the normal metal side. Values of $\sigma(0)$ are much closer to 1 for these Cd-Pb films and in broad outline the data agree well with the Zn-PbBi proximity sandwiches studied by Guyon *et al.*[4] If the data are fit to the empirical relation $1-\sigma(0) \propto (1-T/T_c)^n$, then these Cd-Pb films give $n=1.5$ whereas Guyon *et al.*[4] found values between 2.3 and 3.0 for Zn-PbBi and Vrba and Woods[2] found values ranging from 1 to 6 for Al-Sn. Indeed, calculations of n based on the McMillan model by Vrba and Woods[2] for our measured values of Γ_S and Γ_N indicate that n should be about 1.5. Overall, the $\sigma(0)$ measurements near T_c are in excellent agreement with MTM.

Density-of-states curves for tunneling into the normal side of the proximity sandwich are also qualitatively similar to the predictions of MTM. As predicted by the model, the low-temperature Cd-Pb density of states, shown in Fig. 4(a), is distinctly higher than that for a Pb-Cd junction having nearly the same energy gap. In fact, at higher temperatures, the normalized conductance measured on the Cd side of the junction rises higher than is predicted for a BCS-like superconductor with same energy gap. In Fig. 4(b), the Cd-Pb and Pb-Cd tunneling results at 2.0 K are compared to thermally broadened BCS curves fitted to the experimental data at $\sigma(0)$. It is clear that the tunneling results are not BCS-like nor do they represent a combination of BCS curves with different energy gaps.

A problem of central importance in any proximity-effect measurement is to establish that the

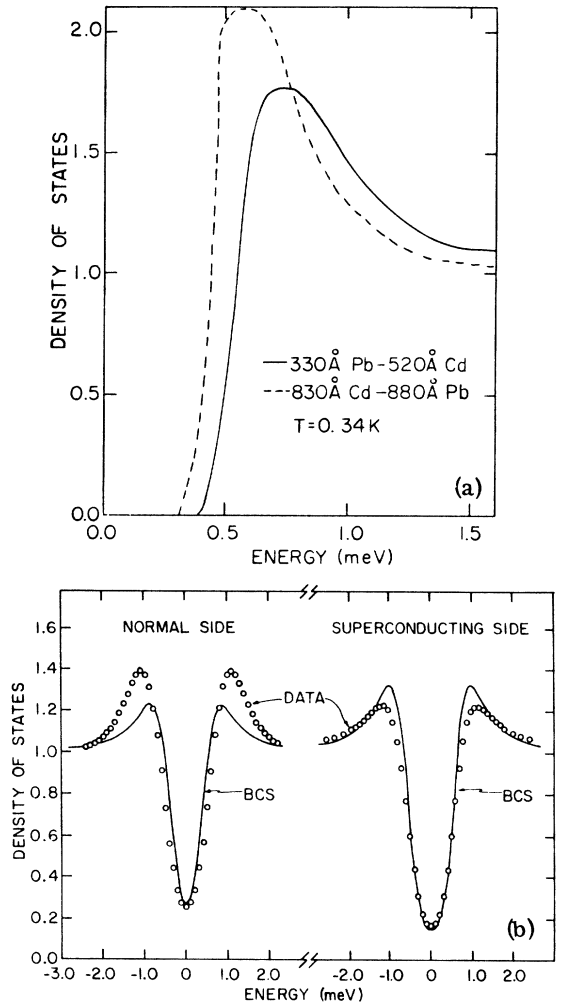

FIG. 4. Comparison of the tunnel conductance for the superconducting (Pb-Cd) and normal (Cd-Pb) sides for two junctions with approximately equal values of Ω. Also shown is a comparison of the tunnel conductance at $T=2.0$ K with BCS curves having the same $\sigma(0)$. Energies are measured from the aluminum gap edge which is 0.18 meV from the Fermi energy.

junction has a genuine layer character rather than being an alloy or being islands of one metal imbedded in the other. There are a number of reasons why we believe these junctions are indeed laminar composites. First, there is a well-defined energy gap Ω with no states in the gap. If there were pinholes in the Pb which are filled with Cd then one would expect additional single-particle tunneling at zero bias associated with tunneling between the Al and the Cd. None is observed. Second, extensive scanning electron microscopy work with laminar Pb-Cd shows that the Pb and Cd regions are stable even at room temperature. Therefore, interdiffusion and alloying is not a problem. Third, and probably most important, is that the tunneling density of states for both the Pb-Cd and for the Cd-Pb films are in agreement with the MTM predictions in most major features. If the junctions were either alloys or islands of one metal in a matrix of the other metal, one would not expect this close agreement with theory for both Pb-Cd and Cd-Pb. For these reasons, we believe the junctions are predominantly laminar form and are relatively free from defects.

For energies up to 2 meV, lifetime broadening is the major factor controlling the shape of the density-of-states curve. As was pointed out by Fulde and Maki,[16] there are some strong similarities between the lifetime effects associated with the proximity effect and those associated with magnetic impurity scattering. In order to compare and contrast these two pair-breaking effects, we plot both T_c/T_{cp} and $\Omega/\Delta^P(0)$ as a function of the reduced lifetime broadening $\Gamma_S/\Delta^P(0)$ on Fig. 5. For the parameters of these particular films, the dependence of T_c on Γ_N is rather small and the transition temperature closely follows the Abrikosov-Gor'kov (AG) prediction. Indeed, in this range of Γ_S and Γ_N, MTM and AG are very close. The energy gap Ω, however, is depressed somewhat faster than AG predicts for the 950-, 670-, and 500-Å films. As shown in Fig. 3(b),

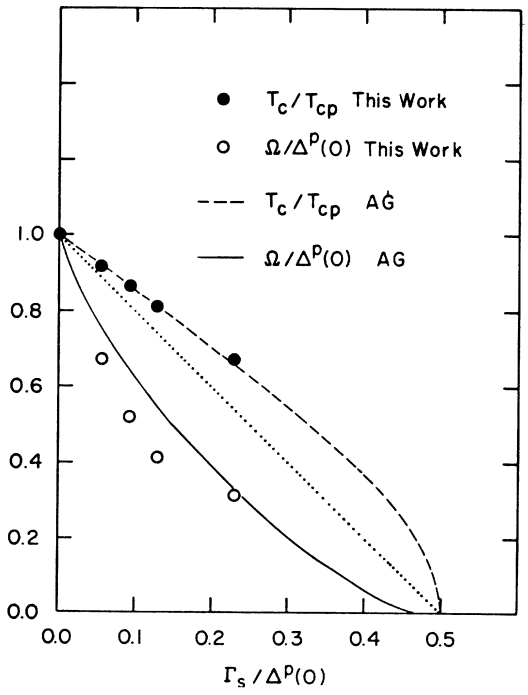

FIG. 5. Comparison of proximity data with the AG theory which describes lifetime-broadening effects arising from magnetic impurity scattering. The dotted line is simply a linear reference line.

MTM predicts an even smaller Ω, so the data lie between the MTM and AG predictions. For the case of the 330-Å film where Γ_S is rather large, the value of Ω is again close to AG. The two main differences between the proximity and the magnetic impurity lifetime-broadening effects are the negative curvature on the steeply rising portion of the σ vs ω curve and the fact that the experimental values of Ω are lower than AG[17] predicts. Many of the features predicted by MTM in the energy range from 0 to 1.5 meV are shown qualitatively by the data but there are some quantitative differences. At energies above 1.5 meV, MTM and AG both give essentially the BCS result.

C. Phonon structure

To make a detailed study of the phonon-induced structure in the density of states, it is helpful to cast the data as a ratio $\sigma(\omega)/\sigma_{BCS}$ where σ_{BCS} is the conductance associated with a BCS density of states[18] for an energy gap equal to E_p. As shown by Fig. 6, the deviations from BCS for an unbacked 670-Å film are about 6% in accord with previous work.[8,19] We find, in fact, that the phonon structure for the unbacked films does not change from the bulk structure by more than a few percent as the thickness decreases. An overlay of 500 Å of Cd, however, sharply reduces the magnitude of the structure in accord with the usual finding[8] that the magnitude of the structure scales with the square of the transition temperature. If the magnitude of the structure at the longitudinal phonon peak is characterized by the parameter δ_L

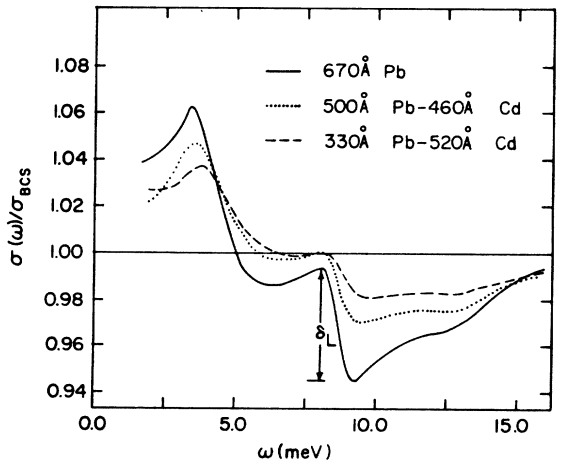

FIG. 6. Variation of the phonon-induced structure in the tunneling density of states as d_S diminishes. The parameter δ_L measures the magnitude of the phonon-induced structure at the longitudinal peak. The solid curve is an unbacked Pb film.

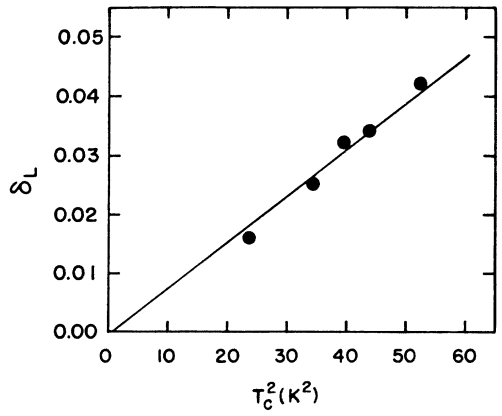

FIG. 7. A plot showing that the deviation of the conductance from BCS is approximately linear in T_c^2.

(also in Fig. 6), then the value of δ_L is fairly close to proportional to T_c^2 as shown in Fig. 7.

A second aspect of the phonon structure is that the position in energy of both the longitudinal and that transverse structure, 4.4 and 8.4 meV, is nearly independent of the thickness of the Pb film and hence the value of Γ_S. For the 330-Å junction, Ω is about one-fourth as large as the bulk Pb zero-temperature pair potential $\Delta^P(0)$, and there are no major changes in the energies at which the phonon structure occur. A search was made for additional structure near the Debye energy of Cd at about 16 meV, but no such structure was observed in any of these Pb-Cd samples to a precision of 0.01%. For the unbacked Pb films, the inversion of the phonon structure using the McMillan unfolding program is rather straightforward and the earlier data[8] are confirmed by these results. We find an $\alpha^2(\omega)F(\omega)$ with Van Hove singularities at the proper energies, an electron-phonon coupling constant $\lambda = 1.51$, a Coulomb repulsion constant $\mu^* = 0.131$, and an average phonon frequency of $\langle\omega\rangle = 5.34$ meV. The control junction parameters are listed in Table I.

Unfolding the proximity data is more complicated than unfolding the data for the unbacked films. The presence of Cd adjacent to the Pb gives a pair potential which is not uniform across the film and the original unfolding procedure requires some modification. As yet, there is no self-consistent theory which gives the energy-dependent pair potential and the density of states as a function of $\alpha^2(\omega)F(\omega)$ and μ^*. Indeed, one will not be given here. It is instructive, however, to try a variety of procedures to illustrate the connection between the measured tunnel conductance and model parameters such as $\alpha^2(\omega)F(\omega)$, μ^*, and Γ_S.

To gain some insight into the magnitude of the

unfolding difficulties, the raw data were analyzed for $\alpha^2(\omega)F(\omega)$ and μ^* using the original McMillan program with the pair potential at the gap edge, Δ_0, equal to E_p. For the 330-Å film this yields an $\alpha^2(\omega)F(\omega)$ curve shown by the solid circles of Fig. 8. The peaks in the curve occur at 4.4 and 8.4 meV just as for bulk Pb (dotted curve) and the longitudinal and transverse peak heights are both about 1.0 and 1.2 meV, respectively. The Van Hove singularities are nearly washed out but there is a striking resemblance to bulk Pb. Two differences are the large high-energy tail above 10 meV in the proximity sandwich and the very large value of $\mu^* = 0.52$. The large tail does not occur at the proper energies to be Cd phonons and the very large value of μ^* seems unlikely to be correct. Presumably these features arise because Δ_0 should not be set equal to E_p and because the basic unfolding procedure does not properly account for the additional lifetime broadening due to the escape of electrons into the Cd.

To modify the unfolding procedure to partially account for the escape lifetime effects, we have focused attention on the renormalization factor. Guided by the McMillan tunneling model, we take

$$Z = Z_0 + i\Gamma_S/(\omega^2 - \Omega^2)^{1/2},$$

where Z_0 is the usual strong coupling renormalization[8] and the $i\Gamma_S/(\omega^2 - \Omega^2)^{1/2}$ term follows from MTM Eq. (20), and use this renormalization throughout the unfolding process. The second term in Z contains the broadening term Γ_S, and it has a square-root denominator to account partially for the high density of states near the gap. With this modified unfolding procedure, the $\alpha^2(\omega)F(\omega)$ look much more reasonable than the $\Gamma_S = 0$ case as shown by the solid curve of Fig. 8. The large high-energy tail is substantially reduced but there is very little change in the position and shape of the phonon peaks. The reduction in magnitude of $\alpha^2(\omega)F(\omega)$ below the unmodified result at all frequencies arises because Δ_0, the value of the pair potential at the gap edge, has been chosen to give $\mu^* = 0.13$, a value much smaller than $\mu^* = 0.52$ which arises if $\Delta_0 = E_p$.

In the original planning of this experiment, it was hoped that both λ and μ^* could be evaluated from the data, but it now appears that μ^* might be uncertain by factors of 2 or more. This uncertainty arises because there is no theory which describes $N(\omega)$ near the gap well enough to define Δ_0 in the unfolding program. MTM is probably accurate to 10%, but a small variation in Δ_0 makes an enormous change in μ^*. To illustrate this sensitivity, μ^* is plotted as a function of Δ_0 in Fig. 9 as the open symbols.

For each sample, μ^* was calculated for Δ_0 ranging from $\Delta_0 = E_p$ upward until μ^* was reduced to 0.13. As indicated on Fig. 9, a 3% increase in Δ_0 changes μ^* from 0.13 to roughly 0.26. Because there is no adequate theory for $N(\omega)$ near the gap edge, the value of Δ_0 certainly cannot be determined to an accuracy of 3% and the μ^* parameter is essentially undetermined by the experiment. It might be added parenthetically that lifetime broadening is not the only effect which can make Δ_0 uncertain in this or any other experiment. Many factors, such as sample inhomogeneity or anisotropy, will make the determina-

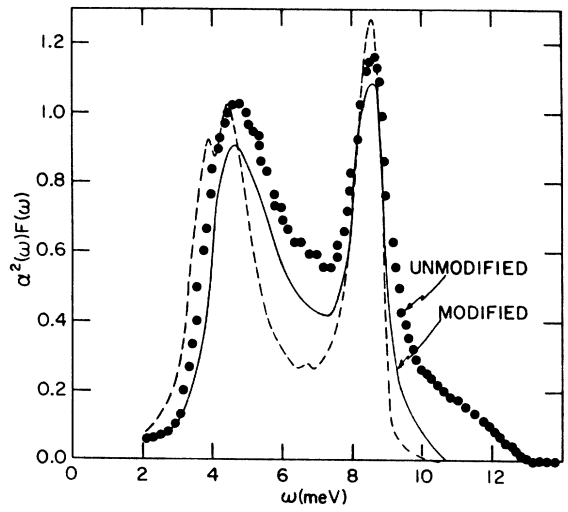

FIG. 8. Values of $\alpha^2(\omega)F(\omega)$ obtained by unfolding with the unmodified Eliashberg equation compared with corresponding values derived with a renormalization factor which accounts for lifetime broadening. The dashed line is the curve for bulk lead.

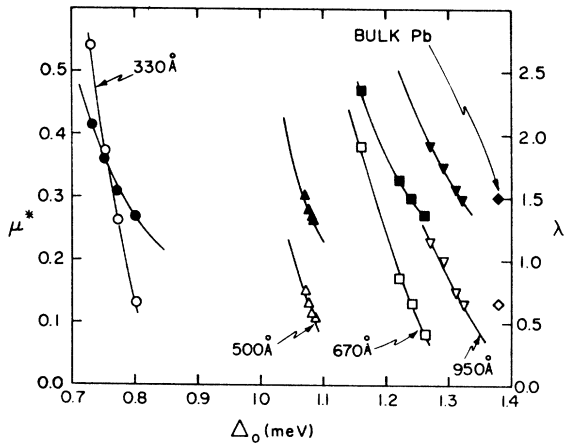

FIG. 9. Dependence of μ^* and λ on the value of the pair potential at the gap edge. The solid symbols are values of λ and go with the right scale. The open symbols are values of μ^* and go with the left scale.

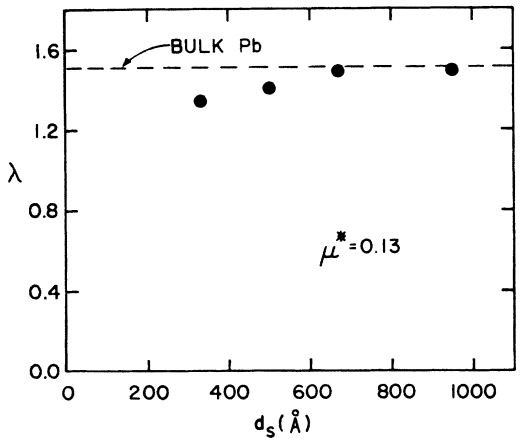

FIG. 10. Thickness dependence of the electron-phonon coupling constant λ for the assumption that $\mu^*=0.13$.

tion of μ^* difficult.

The determination of the electron-phonon coupling constant, $\lambda = \int 2\alpha^2(\omega)F(\omega)\,d\omega/\omega$, is much less difficult. Because μ^* and λ are additive and λ is larger than μ^* by a factor of 10, the percentage error in λ is about 10 times smaller. The solid symbols of Fig. 9 also show the sensitivity of λ to the choice of Δ_0. On the basis of our present understanding of the Coulomb term, we feel that it is unlikely that μ^* changes radically between bulk Pb and a 33 Å thick Pb proximity film and suggest that μ^* might be nearly constant at $\mu^*=0.13$. If this is indeed true, it is interesting to note that λ is also very nearly constant at 1.5 as shown in Fig. 10.

Changes in the spectral function calculated with the modified unfolding program and $\mu^*=0.13$ for various thicknesses shown in Fig. 11. The position of the two main peaks does not change very much but there is a small diminution of the peak heights and a filling in at 6 to 7 meV. The Van Hove singularity at 4 meV is clearly apparent in the 670-Å sample but it is largely gone in the 330-Å sample. Indeed, the 330-Å sample has a much reduced amplitude between 3 and 4 meV and a much enhanced amplitude between 5 and 7 meV. The primary uncertainty in deriving these $\alpha^2(\omega)F(\omega)$ curves arises from the lack of a self-consistent unfolding procedure and the difficulty of determining Δ_0. After experimenting with several procedures, we feel that the curves shown are accurate to about 15%.

An extremely important conclusion is evident from Fig. 11. As the value of d_S diminishes, T_c and the pair potential can drop sharply even though λ and μ^* are essentially constant. The main contribution to the reduction of the pair potential is due to proximity-induced effects which

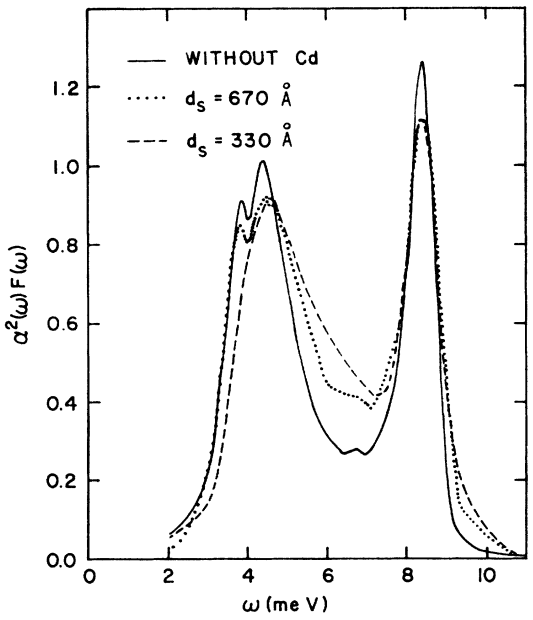

FIG. 11. Calculations of $\alpha^2(\omega)F(\omega)$ using the modified renormalization factor $Z=Z_0+i\,\Gamma_S/(\omega^2-\Omega^2)^{1/2}$ and assuming $\mu^*=0.13$.

are accounted for in the lifetime-broadening term in the pair potential.

IV. CONCLUSIONS

The central result of this work is that the phonon-induced structure in the tunneling density of states for Pb-Cd proximity samples retains essentially the same shape and character as bulk Pb for Pb thicknesses down to 330 Å. The diminution in amplitude of the structure scales with T_c^2.

Near the gap edge, the tunneling density of states for both the Pb-Cd and the Cd-Pb samples reproduce all the major features of the McMillan tunneling model except the low-energy shoulder in the Pb-Cd samples which is supposed to arise from the Cd density of states. Quantitative differences between the model and the data are on the order of 10%. If one assumes that μ^* does not change with decreasing film thickness and modifies the renormalization factor within the spirit of the McMillan model, then one finds that the fundamental electron-phonon parameter λ does not change appreciably as d_S decreases. Rather, the decrease in T_c and Δ arise from the lifetime-broadening term of the renormalization factor.

Finally, it is important to observe that tunneling into the Cd side of the junction gave a much larger energy gap than we anticipated. A 1200 Å thick Cd layer backed with 650 Å of Pb has an energy gap Ω which is 25% of bulk Pb. A further study of the dependence of Ω on d_N for Cd-Pb samples would be very useful.

†Work performed for the U.S. ERDA under Contract No. W-7405-eng-82.

*Permanent address: St. John's University, Collegeville, Minn. 56321.

[1]C. J. Adkins and B. W. Kington, Phys. Rev. 177, 777 (1969).

[2]J. Vrba and S. B. Woods, Phys. Rev. B 3, 2243 (1971); 4, 87 (1971).

[3]J. J. Hauser, H. C. Theuerer, and N. R. Werthamer, Phys. Rev. 136, 637 (1964).

[4]E. Guyon, A. Martinet, S. Mauro, and R. Meunier, Phys. Kondens. Mater. 5, 123 (1966).

[5]T. Claeson and S. Gygax, Solid State Commun. 4, 385 (1966).

[6]J. R. Toplicar and D. K. Finnemore, Solid State Commun. (to be published).

[7]I. Giaever and K. Megerle, Phys. Rev. 122, 1101 (1961)

[8]W. L. McMillan and J. M. Rowell, in *Superconductivity*, edited by R. D. Parks (Marcel Dekker, New York, 1969).

[9]P. G. de Gennes, Rev. Mod. Phys. 36, 225 (1964).

[10]W. L. McMillan, Phys. Rev. 175, 537 (1968).

[11]A. J. Bevolo, E. D. Gibson, J. D. Verhoeven, and D. K. Finnemore, Phys. Rev. B 14, 114 (1976).

[12]J. R. Toplicar, Ph.D. thesis (Iowa State University, 1976) (unpublished).

[13]J. S. Rogers, J. G. Adler, and S. B. Woods, Rev. Sci. Instrum. 35, 208 (1964).

[14]J. J. Hauser, Phys. Rev. 164, 558 (1967).

[15]A. A. Abrikosov and L. P. Gor'kov, Zh. Eksp. Teor. Fiz. 39, 178 (1960) [Sov. Phys.-JETP 12, 1243 (1961)].

[16]P. Fulde and K. Maki, Phys. Rev. Lett. 18, 675 (1965).

[17]S. Skalski, O. Betbeder-Matibet, and P. R. Weiss, Phys. Rev. 136, A1500 (1964).

[18]J. Bardeen, L. N. Cooper, and J. R. Schrieffer, Phys. Rev. 108, 1175 (1951).

[19]W. L. McMillan and J. M. Rowell, Phys. Rev. Lett. 14, 108 (1965).